Acta Cryst. (1981). B37, 1353–1356

Structures of Two Phases of Bis(diethylammonium) Tetrachlorozincate Hydrate

BY D. R. BLOOMQUIST AND R. D. WILLETT

Department of Chemistry, Washington State University, Pullman, Washington 99164, *USA*

(*Received* 27 *May* 1980; *accepted* 20 *January* 1981)

Abstract

$[(C_2H_5)_2NH_2]_2ZnCl_4.xH_2O$ undergoes a first-order structural phase transition at 333 K. The partially dehydrated salt undergoes a phase transition at 308 K. The crystal structures of the room-temperature and high-temperature phases of a partially dehydrated crystal have been determined. The room-temperature phase is monoclinic, Pn, with $a = 10{\cdot}633\ (3)$, $b = 11{\cdot}608\ (4)$, $c = 7{\cdot}391\ (2)$ Å, $\beta = 91{\cdot}11\ (2)°$, $V = 912{\cdot}1$ Å^3, $\rho = 1{\cdot}343$ ($x = 0{\cdot}75$) Mg m^{-3} and $Z = 2$. The high-temperature phase is orthorhombic, $P2_1nm$, with $a = 10{\cdot}719\ (5)$, $b = 11{\cdot}380\ (6)$, $c = 7{\cdot}405\ (4)$ Å, $V = 903{\cdot}3$ Å^3, $\rho = 1{\cdot}329$ ($x = 0{\cdot}33$) Mg m^{-3}, and $Z = 2$. Final R values were 0·053 and 0·075 for 1189, (all data) and 482 ($F > 2\sigma$) reflections, respectively. Both phases contain discrete, tetrahedral $ZnCl_4^{2-}$ anions, hydrogen bonded together through a complex network involving diethylammonium cations and the water molecules. The high-temperature phase contains a mirror plane perpendicular to the c axis. The cations and water molecule are disordered across this mirror plane. In the low-temperature phase, this mirror plane is missing, the disorder is no longer present, and the β angle increases from 90 to 91·11°. Both phases are polar.

Introduction

As part of a study of structural phase transitions in salts containing the diethylammonium cation (henceforth dea), a study has been undertaken of the hydrated salt $(dea)_2ZnCl_4.xH_2O$. We have been particularly interested in understanding the phase transition of the thermochromic material, $(dea)_2CuCl_4$, which is green at room temperature and yellow above $T_c = 329$ K (Willett, Haugen, Lebsack & Morrey, 1974). The room-temperature structure is surprisingly complex, with *three* independent $CuCl_4^{2-}$ anions in the monoclinic unit cell (Simonsen & Harlow, 1977). Preliminary results in our laboratory have shown that the high-temperature form is also monoclinic, with *two* independent $CuCl_4^{2-}$ anions. Because of initial difficulties in growing crystals of the high-temperature phase of $(dea)_2CuCl_4$, we sought to find an isomorphous structure which was not thermochromic. Since the yellow form of $(dea)_2CuCl_4$ (phase I) is known to contain tetrahedrally coordinated Cu^{II} ions, it was anticipated that replacement of the Cu^{II} ion with another transition-metal ion preferring tetrahedral coordination geometry might produce the desired compound. Several transition metals were selected including Mn^{II}, Co^{II}, Cd^{II}, and Zn^{II}. Diethylamine hydrochloride and the appropriate metal chloride in amounts consistent with $(dea)_2MCl_4$ stoichiometry were dissolved in ethanol. The solutions were allowed to evaporate to dryness in open air at room temperature. Preliminary X-ray photographs indicated that none of the products isolated were isomorphous with the high-temperature phase of $(dea)_2CuCl_4$. It did appear that the Zn salt might have some similarities, so a study was initiated, the results of which are reported in this paper.

The compound grew as small, clear crystals from the ethanol solutions. Elemental analysis of a powdered sample of $(dea)_2ZnCl_4.xH_2O$ stored under desiccant showed 18·3% Zn, 27·1% C, 7·9% N, and 6·7% H in good agreement with the dehydrated salt $(dea)_2ZnCl_4$ with predicted composition of 18·4% Zn, 27·0% C, 7·9% N, and 6·8% H. Subsequent studies (see below) indicated the presence of water of hydration in the structure. The predicted composition of the monohydrate $(dea)_2ZnCl_4.H_2O$ is 17·5% Zn, 25·7% C, 7·5% N and 6·5% H. A sample of partially dehydrated $(dea)_2ZnCl_4.xH_2O$ warmed to 311 K for a few hours showed a 3% loss in weight indicating that the dehydration proceeds rapidly at elevated temperatures.

A DTA scan run on the Zn^{II} compound described above showed two endothermic peaks indicating a phase transition ($T_c = 333$ K) preceding melting ($T_m = 366$ K) (see Fig. 1). DSC scans with a heating rate of 5° min^{-1} on partially dehydrated samples showed a broad endothermic transition, first deviating from the baseline at 298 K and centered at 308 K. ΔH_{trans} was estimated from integration of the DSC peak to be approximately $5{\cdot}9 \pm 0{\cdot}8$ kJ mol^{-1}. This indicates that the stability of the low-temperature phase is dependent on the amount of water in the lattice. Partial dehydration also lowers the melting point from 366 to 341 K.

Powder X-ray diffraction patterns were taken below and above the transition temperature. The diffraction patterns were similar but showed distinct differences in

0567-7408/81/071353-04$01.00

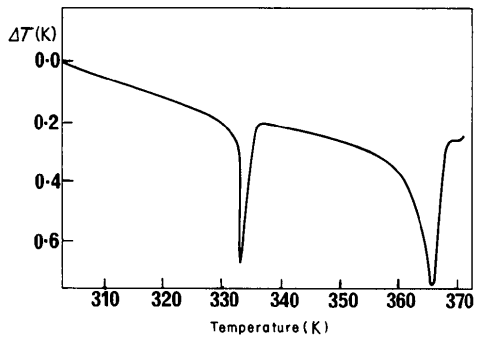

Fig. 1. DTA scan for $(dea)_2ZnCl_4.xH_2O$.

position and intensity of several lines. Due to the presence of a structural phase transition, a complete crystallographic study of the compound was undertaken. Crystals of the compound were found to be extremely fragile and quite hygroscopic, forming a liquid surface layer under moderately humid conditions. Slight pressure applied to a single crystal caused severe twinning visible under the polarizing microscope. The twinning occurred along parallel planes with alternating zones polarizing simultaneously. Crystals with as many as ten alternating zones gave zero-order Weissenberg photographs characteristic of twofold twinning. All crystallographic calculations were carried out with a local program library (Anderson, 1971; Caputo, 1975).

Although no single crystals could be found, a crystal suitable for data collection was located and mounted. The crystal dimensions were 0·37 mm (**a** direction), 0·13 mm (**b** direction), and 0·33 mm (**c** direction). An ω scan across the 004 reflection in the a^*c^* plane holding 2θ fixed showed two peaks separated by 2·2° indicating twinning about the c^* axis. The intensity of the smaller of the two peaks was less than 2% of the larger peak. A total of 1189 unique reflections were collected on an automated Picker four-circle diffractometer with $4° < 2\theta < 45°$, of which 1010 had an intensity greater than 3σ. Intensity data were collected using Zr-filtered Mo $K\alpha$ radiation with a θ–2θ step scan of 1·8° and 3·0 s counting time per step. Background was counted for 15 s before and after each scan. The standard deviation of each reflection was calculated using $\sigma^2(I) = TC + BG + (0{\cdot}03I)^2$, where TC is total counts, BG is background counts, and $I = TC - BG$. Three standard reflections were monitored every 41 reflections and the data were corrected for linear decay. Lorentz–polarization and absorption corrections were applied using $\mu = 3{\cdot}88$ mm^{-1}. Direct-methods probability statistics indicated a non-centrosymmetric structure confirming *Pn* as the space group.

Using a gas-flow temperature controller, the same crystal was warmed slowly to 306 K while the 004 reflection was monitored. Its intensity and that of its twinned counterpart gradually decayed to background over a period of about 5 min as a new peak directly between the two portions of the twin grew in. The new peak corresponds to the c^* axis of a new orthorhombic crystal system with an intensity roughly two-thirds that of the monoclinic 004 reflection. The intensity of the orthorhombic 004 reflection is very temperature-dependent showing a maximum at about 307 K. At temperatures below 307 K, the intensity drops very rapidly to background and above 307 K decreases slowly with increasing temperature due to increased thermal motion. A temperature of 308 ± 1 K was maintained at the crystal during the data collection. No attempt was made to shield the crystal from the atmosphere.

A total of 574 unique reflections with $4° < 2\theta < 42°$ were collected as described above except that a 2·0° θ–2θ scan was used. All reflections were corrected for linear decay, absorption, and Lorentz–polarization. Structural refinement was completed on a data set containing 482 reflections with $F > 2\sigma$. Direct-methods probability statistics were used to verify that the 308 K phase was still non-centrosymmetric.

The $ZnCl_4$ moiety of the room-temperature phase was determined using a Patterson synthesis and the dea atoms were easily located from a Fourier map phased on the heavy atoms. A data set with reflections less than 3σ omitted was used for all least squares except for the final refinement. The structure refinement proceeded normally to a conventional R factor of 0·072 ($R = \sum||F_o| - |F_c||/\sum|F_o|$) with all the $(dea)_2ZnCl_4$ atoms refined using anisotropic thermal parameters. A single large peak was observed on the difference map indicating the presence of a water molecule in the lattice. Including an O atom with anisotropic thermal parameters improved the refinement to $R = 0{\cdot}049$. H atoms were included in their calculated positions with the orientation of the methyl protons being determined from a difference map. A final refinement using a full data set holding all H parameters fixed converged to an R factor of 0·055 and a weighted R factor of 0·045. An R factor of 0·045 was achieved omitting reflections with $F < 3{\cdot}0\sigma$. A slightly better refinement ($R = 0{\cdot}053$, $R_w = 0{\cdot}043$) was obtained by varying the occupancy of the O atom leading to a stoichiometry of $(dea)_2ZnCl_4.0{\cdot}75H_2O$. Final positional and thermal parameters are listed in Table 1 and bond distances and angles are summarized in Table 3. Fig. 2 is a stereo *ORTEP* drawing of the unit cell as viewed from the **a** direction.

With the exception of Cl(3), all atom positions for the high-temperature orthorhombic phase were located by projection of the monoclinic positions onto the corresponding mirror planes. The Cl(3) coordinates were taken as the average of the coordinates of the corresponding atoms [Cl(3) and Cl(4)] of the low-

Table 1. *Positional and thermal parameters for the non-hydrogen atoms of the room-temperature phase of* $[(C_2H_5)_2NH_2]_2ZnCl_4.0{\cdot}75H_2O$

U_{eq} was calculated using the formula $U_{eq} = \frac{1}{3}\sum_i\sum_j U_{ij}a_i^*a_j^*\mathbf{a}_i.\mathbf{a}_j$. The estimated standard deviation was taken as the mean deviation of U_{11}, U_{22}, and U_{33}.

	x	y	z	U_{eq} (Å^2)
Zn	0·0	0·2518 (1)	0·0	0·0600 (7)
Cl(1)	0·2095 (3)	0·2553 (3)	0·0229 (5)	0·093 (2)
Cl(2)	−0·0842 (3)	0·4295 (3)	−0·0406 (4)	0·082 (2)
Cl(3)	−0·0712 (4)	0·1424 (3)	−0·2362 (4)	0·088 (2)
Cl(4)	−0·0819 (3)	0·1723 (3)	0·2535 (4)	0·077 (2)
C(*A*1)	0·155 (1)	0·669 (2)	0·056 (3)	0·14 (2)
C(*A*2)	0·240 (2)	0·579 (1)	−0·009 (2)	0·10 (1)
N(*A*)	0·3724 (9)	0·6095 (7)	0·023 (1)	0·070 (6)
C(*A*3)	0·463 (1)	0·522 (1)	−0·032 (2)	0·10 (1)
C(*A*4)	0·593 (1)	0·563 (1)	−0·001 (2)	0·12 (1)
C(*B*1)	0·067 (2)	0·819 (2)	0·555 (3)	0·17 (1)
C(*B*2)	0·099 (2)	0·925 (1)	0·479 (2)	0·12 (1)
N(*B*)	0·204 (1)	−0·009 (1)	0·553 (2)	0·072 (7)
C(*B*3)	0·238 (2)	0·097 (1)	0·483 (2)	0·12 (1)
C(*B*4)	0·345 (1)	0·159 (1)	0·540 (2)	0·12 (1)
O	0·201 (1)	−0·016 (1)	0·952 (2)	0·18 (1)

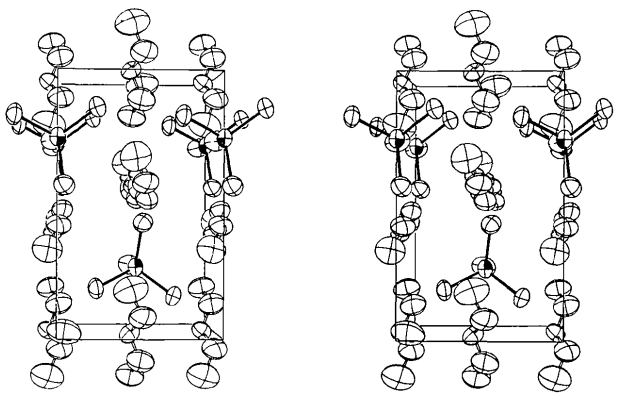

Fig. 2. Stereographic illustration of the unit cell of the room-temperature phase as viewed from the **a** direction.

temperature structure, which become equivalent in the high-temperature form. The best refinement was achieved by placing all dea atoms on the mirror planes and allowing anisotropic thermal parameters to compensate for dynamic disorder across the mirror planes. Least-squares refinement failed to converge for more complicated ordered anisotropic dea models, partly due to the limited intensity data available. No attempt was made to include hydrogens in the refinement. The position of the O atom was located from a difference Fourier map and was found to be disordered and smaller in intensity than was expected. The oxygen was placed slightly off the mirror plane with isotropic thermal parameters and the position and multiplier were allowed to vary. The best refinement indicated a structure of stoichiometry $(dea)_2ZnCl_4.0{\cdot}33H_2O$ suggesting further partial dehydration. Using a data set omitting reflections with $F < 2\sigma$, a final convergence of $R = 0{\cdot}075$ was obtained with a weighted convergence of $R_w = 0{\cdot}063$. Final thermal and positional parameters for the 308 K phase are given in Table 2.* Distances and angles for both phases are compared in Table 3. The unreasonably large angles and short bond lengths in the dea cations, especially cation *B*, are the result of the inability to fit dynamic disorder with anisotropic thermal parameters restricted by mirror symmetry. The unit cell is drawn in stereo in Fig. 3. All atoms are drawn with 50%

* Lists of structure factors and anisotropic thermal parameters for both phases and H atom parameters for the room-temperature phase have been deposited with the British Library Lending Division as Supplementary Publication No. SUP 36005 (10 pp.). Copies may be obtained through The Executive Secretary, International Union of Crystallography, 5 Abbey Square, Chester CH1 2HU, England.

Table 2. *Positional and thermal parameters for the high-temperature phase of* $[(C_2H_5)_2NH_2]_2ZnCl_4.0{\cdot}33H_2O$

U_{eq} was calculated using the formula $U_{eq} = \frac{1}{3}\sum_i\sum_j U_{ij}a_i^*a_j^*\mathbf{a}_i.\mathbf{a}_j$. The estimated standard deviation was taken as the mean deviation of U_{11}, U_{22}, and U_{33}.

	x	y	z	U_{eq} (Å^2)
Zn	0·0	0·2500	0·0	0·109 (3)
Cl(1)	0·2117 (9)	0·2470 (8)	0·0	0·175 (9)
Cl(2)	−0·077 (1)	0·4293 (8)	0·0	0·172 (8)
Cl(3)	−0·0709 (8)	0·1535 (5)	0·2446 (7)	0·141 (6)
C(*A*1)	0·164 (4)	0·666 (3)	0·0	0·17 (4)
C(*A*2)	0·242 (4)	0·584 (3)	0·0	0·17 (4)
N(*A*)	0·376 (3)	0·615 (2)	0·0	0·11 (2)
C(*A*3)	0·459 (5)	0·510 (3)	0·0	0·16 (4)
C(*A*4)	0·594 (5)	0·552 (3)	0·0	0·19 (5)
C(*B*1)	0·069 (5)	0·836 (4)	0·5000	0·19 (4)
C(*B*2)	0·114 (5)	0·930 (4)	0·5000	0·25 (6)
N(*B*)	0·201 (3)	0·009 (4)	0·5000	0·18 (4)
C(*B*3)	0·242 (5)	0·097 (4)	0·5000	0·31 (7)
C(*B*4)	0·337 (4)	0·174 (4)	0·5000	0·17 (4)
O	0·218 (7)	0·015 (5)	0·071 (9)	0·089

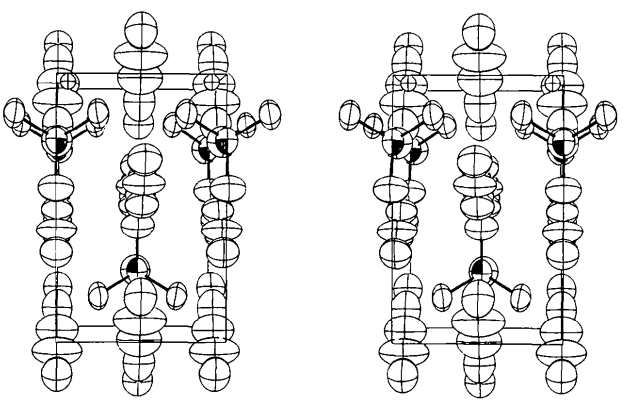

Fig. 3. Stereographic illustration of the unit cell of the high-temperature phase as viewed from the **a** direction.

Table 3. *Comparison of bond distances* (Å) *and angles* (°) *for* $(dea)_2ZnCl_4.H_2O$ *phases* I *and* II

Phase II (293 K)		Phase I (308 K)	
Zn–Cl(1)	2·231 (3)	Zn–Cl(1)	2·27 (1)
Zn–Cl(2)	2·266 (3)	Zn–Cl(2)	2·199 (9)
Zn–Cl(3)	2·277 (3)	Zn–Cl(3)	2·250 (6)
Zn–Cl(4)	2·277 (3)		
C(*A*1)–C(*A*2)	1·47 (2)	C(*A*1)–C(*A*2)	1·25 (4)
C(*A*2)–N(*A*)	1·47 (2)	C(*A*2)–N(*A*)	1·48 (4)
N(*A*)–C(*A*3)	1·46 (1)	N(*A*)–C(*A*3)	1·49 (4)
C(*A*3)–C(*A*4)	1·47 (2)	C(*A*3)–C(*A*4)	1·53 (5)
C(*B*1)–C(*B*2)	1·40 (2)	C(*B*1)–C(*B*2)	1·17 (5)
C(*B*2)–N(*B*)	1·45 (2)	C(*B*2)–N(*B*)	1·30 (5)
N(*B*)–C(*B*3)	1·38 (2)	N(*B*)–C(*B*3)	1·09 (5)
C(*B*3)–C(*B*4)	1·40 (2)	C(*B*3)–C(*B*4)	1·35 (5)
O–Cl(1)	3·19(1)	O–Cl(1)	2·69 (5)
O–Cl(4)	3·30 (1)	O–Cl(3)	3·26 (7)
O–N(*B*)	2·95 (2)	O–N(*B*)	3·18 (6)
N(*A*)–Cl(4)	3·26 (1)	N(*A*)–Cl(3)	3·29 (2)
N(*A*)–Cl(2)	3·28 (1)	N(*A*)–Cl(2)	3·771 (5)
N(*B*)–Cl(4)	3·29 (1)	N(*B*)–Cl(3)	3·56 (3)
Cl(1)–Zn–Cl(2)	112·6 (1)	Cl(1)–Zn–Cl(2)	112·8 (3)
Cl(1)–Zn–Cl(3)	112·6 (1)	Cl(1)–Zn–Cl(3)	109·3 (2)
Cl(1)–Zn–Cl(4)	110·0 (1)	Cl(2)–Zn–Cl(3)	109·1 (2)
Cl(2)–Zn–Cl(3)	106·4 (1)	Cl(3)–Zn–Cl(3)	107·2 (3)
Cl(2)–Zn–Cl(4)	108·7 (1)		
Cl(3)–Zn–Cl(4)	106·1 (1)		
C(*A*1)–C(*A*2)–N(*A*)	112 (1)	C(*A*1)–C(*A*2)–N(*A*)	118 (4)
C(*A*2)–N(*A*)–C(*A*3)	115 (1)	C(*A*2)–N(*A*)–C(*A*3)	113 (3)
N(*A*)–C(*A*3)–C(*A*4)	111 (1)	N(*A*)–C(*A*3)–C(*A*4)	108 (3)
C(*B*1)–C(*B*2)–N(*B*)	121 (2)	C(*B*1)–C(*B*2)–N(*B*)	158 (6)
C(*B*2)–N(*B*)–C(*B*3)	122 (1)	C(*B*2)–N(*B*)–C(*B*3)	157 (6)
N(*B*)–C(*B*3)–C(*B*4)	124 (2)	N(*B*)–C(*B*3)–C(*B*4)	154 (6)

probability ellipsoids except for the oxygen of phase I (308 K) which is drawn isotropic with $B = 3{\cdot}0$ Å^2. No H atoms are included in the drawings.

Discussion

Both phases of $(dea)_2ZnCl_4.H_2O$ contain tetrahedral $ZnCl_4^{2-}$ anions, all angles being within 3·5° of the tetrahedral angle. The shortest Zn–Cl bond in the 293 K phase [2·231 (3) Å] becomes the longest in the 308 K phase [2·28 (1) Å] demonstrating that considerable rearrangement of the hydrogen-bonding scheme accompanies the phase transition. A water molecule is loosely trapped within the lattice of freshly prepared crystals, accounting for the unusual non-centrosymmetric structure. Partial dehydration of the compound occurs at room temperature without damage to the crystalline properties. All Cl atoms except Cl(3) participate in a rather complex hydrogen-bonding network involving the water molecule and the N atoms.

The room-temperature phase contains a pseudo-mirror plane perpendicular to the *c* axis which intersects the thermal ellipsoids of all atoms except Cl(3) and Cl(4). The bond distances and angles of dea cation *A* are characteristic of normal cation geometry while cation *B* contains several relatively short bonds [1·38 (2) Å] and all angles are significantly larger than the tetrahedral angle (greater than 120°). Thermal parameters for cation *B* show large thermal motion at room temperature accounting for the deviations in bond distances and angles.

Above 308 K, a shift to an orthorhombic cell introduces crystallographic mirror planes perpendicular to the *c* axis causing Cl(3) and Cl(4) to become equivalent. The electron density map indicates severe disorder in the O atom with the highest density corresponding to a dynamic disorder across the mirror plane. The Cl atoms also show increased thermal motion indicating a weakening of the hydrogen-bonding structure. The dehydration process occurs much more rapidly in the orthorhombic phase, due to the increased mobility of the water molecule accompanying the partial collapse of the hydrogen-bonding network.

In the 308 K phase both cations are restricted to lie on crystallographic mirror planes. Bond distances and angles for cation *A* at 308 K are characteristic of increased thermal motion with the largest thermal parameters corresponding to the direction perpendicular to the mirror planes. The electron density map for cation *B* shows broad poorly defined regions of electron density corresponding to excessive torsional motion about the cation axis. Anisotropic temperature factors restricted by mirror symmetry provide a poor model for this type of motion resulting in the unreasonably short bond distances and large angles. Considerable thermal motion resulting in severely restricted diffracted intensity data renders refinements involving more complicated cation models impossible.

References

ANDERSON, D. N. (1971). PhD Thesis, Washington State Univ.

CAPUTO, R. E. (1975). PhD Thesis, Washington State Univ.

SIMONSEN, S. H. & HARLOW, R. L. (1977). *Am. Crystallogr. Assoc. Abstr.* **5**, No. 1, Abstr. HN-5.

WILLETT, R. D., HAUGEN, J. A., LEBSACK, J. & MORREY, J. (1974) *Inorg. Chem.* **13**, 2510–2513.